AUT Journal of Mathematics and Computing

AUT J. Math. Comput., 7(1) (2026) 45-61
https://doi.org/10.22060/AJMC.2024.23406.1254

Original Article

Solving the optimum control problem constrained with Volterra integro-differential equations using Chebyshev wavelets and particle swarm optimization

Asiyeh Ebrahimzadeh*

Department of Mathematics Education, Farhangian University, P. O. Box 14665-889, Tehran, Iran

ABSTRACT: To handle a type of optimum control problems (OCP) for systems controlled described by Volterra integro-differential equations (VIDE), we introduce in this study a direct Chebyshev wavelet collocation approach, which is utilized in applied science and engineering. The proposed direct approach turns the OCP into a nonlinear programming (NLP) problem, in which the wavelet coefficients are the optimization variables. To solve the resulting NLP, we use the particle swarm optimization (PSO) technique. In addition, we illustrate the suggested method's convergence. Under certain sufficient conditions, it is shown that a sequence of optimal solutions for the finite-dimensional optimization problems corresponding to $\overline{\mathcal{P}}$ approximates the optimal solution of the original problem $\mathcal{P}$ in a desirable manner. To demonstrate the method's applicability and efficiency, we provide several numerical examples that emphasize the PSO algorithm's effectiveness in solving the resulted NLP.

Review History:

Received:02 August 2024
Revised:20 October 2024
Accepted:17 November 2024
Available Online:01 January 2026

Keywords:

Chebyshev wavelet
Optimal control
Particle swarm optimization
Collocation method
Volterra integro–differential equation

MSC (2020):

49M25; 90C59; 45D05

1. INTRODUCTION

OCP, which is a dynamic optimization problem over a time horizon, plays a substantial role in modeling many phenomena in numerous fields, including Mathematics, Physics, and Medicine [1, 2, 21]. The subtle modeling of many phenomena, especially those with memory effects, leads to the Volterra integral equation (VIE) or VIDE [17]. Solving OCPs of VIDEs is important because these equations effectively model systems with memory effects, where the current state depends on past states, which is common in many physical, biological, and engineering systems. Examples include heat conduction in materials, population dynamics, and economic models. Addressing these problems allows for the design of control strategies that optimize performance, such as minimizing energy consumption or improving resource management, even in complex systems with time delays and nonlinearity. Since analytical solutions are often difficult or impossible to obtain, numerical methods are essential for approximating

*Corresponding author.
E-mail address: a.ebrahimzadeh@cfu.ac.ir (A. Ebrahimzadeh)

solutions. Therefore, studying OCPs for VIDEs is important for both theoretical advancements and practical applications [19].

Research in OCP constrained by VIE or VIDE has seen significant advancements, particularly in addressing nonlinear dynamics. Early works, such as those by Tohidi and Samadi, utilized Legendre polynomials to formulate solutions for nonlinear Volterra integral equations, providing a foundational approach for subsequent studies [25]. Further developments include the application of triangular functions, rationalized Haar wavelet and hybrid pseudo-spectral methods which enhance computational efficiency and accuracy in solving these complex equations [16, 17, 18]. Recent studies have also introduced innovative numerical techniques that leverage polynomial approximations and operational matrices, demonstrating improved convergence properties and robustness in handling weakly singular kernels [7, 20]. The paper in [19] employs a hybrid functions approach to solve optimal control problems associated with integro-differential equations. This method combines the use of hybrid functions with collocation techniques, allowing for the transformation of integro-differential equations into algebraic equations that can be solved numerically. Numerous studies have been conducted on developing, analyzing, and implementing numerical algorithms for solving OCP regulated by VIE or VIDE [6, 10, 11, 16, 17, 18, 19, 25].

In this study, we focus on a specific class of OCPs governed by a VIDE. The problem formulation is as follows:
Problem $\mathcal{P}$: Consider the next class of OCP constrained by a nonlinear VID equation:

$$\min\ \mathcal{J} = \int_{t_0}^{t_f} \mathcal{F}(t, x(t), u(t))dt, \tag{1}$$

subject to

$$x'(t) = a(t)x(t) + b(t)u(t) + \int_{t_0}^{t} \mathcal{K}(t,s)\varphi(x(s))ds, \quad x(t_0) = x_0, \tag{2}$$

where $\mathcal{F}$, $\mathcal{K}$, $a(t)$, $b(t)$ and φ are real-valued functions that possess continuous derivatives with respect to their respective arguments. Suppose that $x(t)$ and $u(t)$ are in Sobolev space, $\mathcal{H}^{l,\infty}(l \geq 2)$. $\varphi(t)$ can be either a continuous nonlinear or linear operator. If the function u is such that the constraints in equation (2) are satisfied, then it is called a feasible control. Let U be the class of all such feasible controls. The significance of OCP governed by VIDEs lies in their widespread applicability in various fields such as physics, engineering, and biology, where systems with memory effects are modeled [7, 20].

Chebyshev wavelets are used in this study to estimate the unknown solutions of the OCP. By using Chebyshev wavelets, the primal OCP is transformed into an NLP, where the wavelet coefficients serve as the optimization variables. To solve the resulting NLP problem, we utilize the PSO algorithm, which is particularly advantageous due to its simplicity in implementation, efficiency in exploring the solution space, and rapid convergence capabilities [23, 26, 27]. Inspired by the collective behavior of birds and fish, PSO leverages group searching strategies to find the optimal solution effectively. We provide some illustrative examples to demonstrate the practical applicability and efficiency of our propounded approach, highlighting how the combination of collocation based on Chebyshev wavelets and PSO can effectively address these optimization challenges.

Since deriving analytical solutions for some OCPs is challenging, numerical direct and indirect techniques are typically employed to determine the optimal solutions for state and control variables. A direct method for solving OCP offers substantial advantages over indirect methods [4]. While indirect methods derive first-order optimality conditions leading to complex boundary-value problems, the direct method discretizes the state and control variables, transforming the OCP into an NLP that can be efficiently solved using techniques like meta-heuristic algorithms [14]. Utilizing Chebyshev wavelets for approximating unknown solutions enhances this approach. Chebyshev wavelets provide excellent approximation capabilities due to their orthogonality and localization properties, allowing for accurate representation of the control and state variables over the problem domain [14]. Additionally, the utilizing of a derivative operational matrix simplifies the differentiation process, converting differential equations in constraints into algebraic equations, thus facilitating more manageable and more precise computation. The method presented in this paper differs from other existing approaches primarily in its combination of Chebyshev wavelet collocation and the PSO algorithm for solving the optimal control problem governed by VIDEs. Unlike traditional methods that rely solely on wavelet-based approximations or numerical integration, this approach directly transforms the continuous-time optimal control problem into a NLP problem using Chebyshev wavelets, where wavelet coefficients are treated as optimization variables. The use of PSO algorithm as a solver for the resulting NLP is particularly innovative, as it leverages the swarm-based search mechanism to efficiently explore the solution space and converge to an optimal solution. The hybridization of direct methods with PSO combines the robustness of meta-heuristic algorithms with the precision of wavelet-based approximations, leading to a highly efficient and accurate solution method for OCPs. These advantages collectively improve the efficiency and applicability of numerical methods in dissolving complex OCPs governed by VIDEs, demonstrating the robustness and effectiveness of the proposed approach. This distinguishes it from other methods that might use classical optimization techniques or purely analytical methods, making it more suitable for problems with complex dynamics and memory effects like those governed by VIDEs.

The structure of this article is as follows: Section 2 discusses the foundational characteristics of the Chebyshev wavelet necessary for our work, including the derivation of the operational matrices for the Chebyshev wavelet. In Section 3, we demonstrate the process of transforming OCP in problem $\mathcal{P}$ into an NLP using the Chebyshev wavelet and introduce the PSO algorithm. Section 4 provides the convergence of the propounded method. Section 5 presents numerical experiments focused on the accuracy of the method for solving Problem $\mathcal{P}$. This study ends with a summary in Section 6.

2. Background Materials and Preliminaries

This section introduces the mathematical preliminaries of the Chebyshev wavelet needed for the following development. Understanding these fundamentals is crucial for effectively applying Chebyshev wavelets in various computational problems. By grasping these concepts, practitioners can leverage the unique properties of Chebyshev wavelets to enhance accuracy and efficiency in numerical simulations.

2.1. Chebyshev Wavelet

Chebyshev wavelets $\Psi_{nm}(t)$ of order m with $n = 1, 2, 3, \dots, 2^k$ and $k \in N$ can be defined on the interval $[0, 1]$ as follows [8]:

$$\Psi_{mn}(t) = \begin{cases} \frac{\alpha_m 2^{\frac{k}{2}}}{\sqrt{\pi}} \mathcal{T}_m(2^{k+1}t - 2n + 1) & \text{if } \frac{n-1}{2^k} \le t \le \frac{n}{2^k} \\ 0 & \text{otherwise} \end{cases}, \tag{3}$$

in which

$$\alpha_m = \begin{cases} \sqrt{2} & m = 0 \\ 2 & m = 1, 2, 3, \dots, M-1 \end{cases}. \tag{4}$$

$\mathcal{T}_m(t)$ show the orthogonal first kind Chebyshev polynomials of degree m with weight function $\mathcal{W}(t) = \frac{1}{\sqrt{1-t^2}}$ defined in the interval $[-1, 1]$, which satisfy in the following recurrence relation:

$$\mathcal{T}_0(t) = 1, \quad \mathcal{T}_1(t) = t, \quad \mathcal{T}_{m+1} = 2t\mathcal{T}_m(t) - \mathcal{T}_{m-1}(t), \quad m = 1, 2, \dots.$$

When dealing with the weight function of Chebyshev wavelets, we defined it as follows:

$$\mathcal{W}_n(t) = \mathcal{W}(2^k t - 2n + 1), \tag{5}$$

to ensure orthogonality over the interval $[0, 1]$. For expanding the function $\mathcal{G}(t)$ defined on $[0, 1]$, we obtain:

$$\mathcal{G}(t) = \sum_{n=1}^{\infty} \sum_{m=0}^{\infty} \mathcal{C}_{nm} \Psi_{nm}(t), \tag{6}$$

where the coefficients $\mathcal{C}_{nm}$ are determined by:

$$\mathcal{C}_{nm} = \langle \mathcal{G}(t), \Psi_{nm}(t) \rangle_{\mathcal{W}_n}, \tag{7}$$

and $\langle \cdot, \cdot \rangle_{\mathcal{W}_n}$ show the inner product with respect to the weight function $\mathcal{W}_n$ as defined in equation (5). By considering a truncated series in equation (6), we have:

$$\mathcal{G}(t) \simeq \sum_{n=1}^{2^{k-1}} \sum_{m=0}^{M-1} \mathcal{C}_{nm} \Psi_{nm}(t) = \mathcal{C}^T \Psi(t), \tag{8}$$

in which $\mathcal{C}$ and Ψ are $2^{k-1}M \times 1$ vectors defined by:

$$\mathcal{C} = [\mathcal{C}_{10}, \mathcal{C}_{11}, \dots, \mathcal{C}_{1,M-1}, \mathcal{C}_{20}, \dots, \mathcal{C}_{2,M-1}, \dots, \mathcal{C}_{2^{k-1},0}, \dots, \mathcal{C}_{2^{k-1},M-1}]^T, \tag{9}$$

$$\Psi(t) = [\Psi_{10}, \Psi_{11}, \dots, \Psi_{1,M-1}, \Psi_{20}, \dots, \Psi_{2,M-1}, \dots, \Psi_{2^{k-1},0}, \dots, \Psi_{2^{k-1},M-1}]^T. \tag{10}$$

2.2. The derivative operational matrix of Chebyshev wavelet

The operational matrix of the derivative has significant attention due to its properties in facilitating the solution process for dissolving differential or integro-differential equations by transmuting the problem into a system of algebraic equations. For simplicity and accuracy in handling nonlinear equations, the operational matrix of the derivative is applied instead of the integration matrix. By differentiating the vector $\Psi(t)$ in equation (10), it can be expressed exactly as:

$$\frac{d\Psi(t)}{dt} = \mathcal{D}\Psi(t), \tag{11}$$

in which $\mathcal{D}$ is the $2^{k-1}M$ operational matrix of derivative, defined as follows [12]:

$$\mathcal{D} = \begin{pmatrix} \mathcal{M} & 0 & \dots & 0 \\ 0 & \mathcal{M} & \dots & 0 \\ \vdots & \vdots & \ddots & \vdots \\ 0 & 0 & 0 & \mathcal{M} \end{pmatrix}, \tag{12}$$

where $\mathcal{M}$ is an $M \times M$ matrix with elements defined by:

$$\mathcal{M}_{rs} = \begin{cases} 2^{k+1}\sqrt{\frac{c_{r-1}}{c_{s-1}}}, & \text{if } r = 2, \dots, M,\ s = 1, \dots, r-1 \text{ and } (r+s) \text{ is odd}, \\ 0, & \text{otherwise} \end{cases} \tag{13}$$

Constants c_i in equation (13) are specified in [12]. The Chebyshev wavelet operational matrix of derivative for $k = 2$ and $M = 4$ is given by:

$$\mathcal{D} = 8 \cdot \begin{pmatrix} 0 & 0 & 0 & 0 & 0 & 0 & 0 & 0 \\ \frac{1}{\sqrt{2}} & 0 & 0 & 0 & 0 & 0 & 0 & 0 \\ 0 & 2 & 0 & 0 & 0 & 0 & 0 & 0 \\ 3 \cdot \frac{1}{\sqrt{2}} & 0 & 3 & 0 & 0 & 0 & 0 & 0 \\ 0 & 0 & 0 & 0 & 0 & 0 & 0 & 0 \\ 0 & 0 & 0 & 0 & \frac{1}{\sqrt{2}} & 0 & 0 & 0 \\ 0 & 0 & 0 & 0 & 0 & 2 & 0 & 0 \\ 0 & 0 & 0 & 0 & 3 \cdot \frac{1}{\sqrt{2}} & 0 & 3 & 0 \end{pmatrix}.$$

In several studies, the derivative operational matrix have been applied to solve various types of differential equations [22].

3. Implementation of the Proposed Method

In addressing problem $\mathcal{P}$, without loss of generality, we set $t_0 = 0$ and $t_f = 1$. This simplification is feasible due to the ability to transform any closed interval linearly into another. This section elaborates on the discretization process for problem $\mathcal{P}$ and the methodology for solving it. The approach involves discretizing both the cost functional in equation (1) of problem $\mathcal{P}$ and the constrained integro-differential equation given in (2). Subsequently, the PSO algorithm is applied to dissolve the resulting NLP. By combining discretization techniques with the PSO algorithm, we can efficiently solve the original continuous-time optimal control problem (1)-(2) and obtain an approximate solution satisfying the constraints and minimizing the cost functional. The procedure is detailed as follows:

3.1. Collocation Methodology

By approximating the functions $x(t)$, $u(t)$, and $x'(t)$ using Chebyshev wavelets. This can be expressed as:

$$x(t) \approx \overline{\mathcal{X}}(t) = \mathcal{X}^T\Psi(t), \quad u(t) \approx \overline{\mathcal{U}}(t) = \mathcal{U}^T\Psi(t), \quad x'(t) \approx \overline{\mathcal{X}}'(t) = \mathcal{X}^T\mathcal{D}\Psi(t), \tag{14}$$

where

$$\mathcal{X} = [\mathcal{X}_{10}, \mathcal{X}_{11}, \dots, \mathcal{X}_{1M-1}, \dots, \mathcal{X}_{2^{k-1}0}, \dots, \mathcal{X}_{2^{k-1}M-1}]^T,$$
$$\mathcal{U} = [\mathcal{U}_{10}, \mathcal{U}_{11}, \dots, \mathcal{U}_{1M-1}, \dots, \mathcal{U}_{2^{k-1}0}, \dots, \mathcal{U}_{2^{k-1}M-1}]^T,$$

with Ψ introduced in (10), $\mathcal{X}$ and $\mathcal{U}$ as the unknown column vectors to be determined, and $\mathcal{D}$ as the derivative operational matrix introduced in equation (12) of section 2.2. Substituting (14) into the system dynamics (2) and collocating at points t_p, we derive:

$$\mathcal{X}^T\mathcal{D}\Psi(t_p) = a(t_p)\mathcal{X}^T\Psi(t_p) + b(t_p)\mathcal{U}^T\Psi(t_p) + \int_0^{t_p} \mathcal{K}(t_p, s)\varphi(x(s))ds, \quad \mathcal{X}^T\Psi(0) = x(0), \quad p = 1, 2, \dots, 2^{k-1}M \tag{15}$$

in which t_p may be selected as Gauss-Chebyshev (GC) nodes, Gauss-Legendre (GL) nodes-specifically, the zeros of Legendre polynomials-or as central nodes. The GL or GC nodes must be transformed into the interval $[0,1]$.

For approximating the integral term in (15) using GL quadrature, $2^{k-1}M$ intervals $[0,t_p]$ are transformed to the interval $[-1,1]$ via $s=\frac{t_p}{2}(\tau+1)$, $p=1,\ldots,2^{k-1}M$. This yields:

$$\begin{aligned}&-\mathcal{X}^T\mathcal{D}\Psi(t_p)+a(t_p)\mathcal{X}^T\Psi(t_p)+b(t_p)\mathcal{U}^T\Psi(t_p)\\&\qquad+\frac{t_i}{2}\sum_{j=0}^{\mathcal{N}}\mathcal{W}_j\left(\mathcal{K}\left(t_p,\frac{t_p}{2}(\tau_j+1)\right)\varphi\left(\mathcal{X}^T\Psi\left(\frac{t_p}{2}(\tau_j+1)\right)\right)\right)=0,\quad \mathcal{X}^T\Psi(0)=x(0),\end{aligned}\tag{16}$$

where τ_j's for $1\le j\le\mathcal{N}=2^kM$ are GL nodes, and $\mathcal{W}_j$'s are the corresponding weights, given by:

$$\mathcal{W}_j=\frac{2}{(1-\tau_j^2)[\mathcal{L}'_{N+1}(\tau_j)]^2},\quad j=0,1,\ldots,\mathcal{N}.\tag{17}$$

Now, let's discretize the cost functional described in (1). After a suitable interval transformation, we employ the GL quadrature

$$\begin{aligned}\int_0^1\mathcal{F}(t,x(t),u(t))dt&=\frac{1}{2}\int_{-1}^{1}\mathcal{F}\left(\frac{\tau+1}{2},x\left(\frac{\tau+1}{2}\right),u\left(\frac{\tau+1}{2}\right)\right)d\tau\\&\approx\frac{1}{2}\sum_{i=1}^{\mathcal{N}}\mathcal{F}\left(\frac{\tau_j+1}{2},x\left(\frac{\tau_j+1}{2}\right),u\left(\frac{\tau_j+1}{2}\right)\right)\mathcal{W}_j.\end{aligned}\tag{18}$$

By approximating $u(t)$ and $x(t)$ according to (14), we obtain:

$$\mathcal{J}_{\mathcal{N}}(X,U)=\frac{1}{2}\sum_{i=1}^{\mathcal{N}}\mathcal{F}\left(\frac{\tau_j+1}{2},X^T\Psi\left(\frac{\tau_j+1}{2}\right),U^T\Psi\left(\frac{\tau_j+1}{2}\right)\right)\mathcal{W}_j.\tag{19}$$

Following [9], we suggest the following relaxation to ensure the discretization's feasibility:

$$\begin{aligned}\Bigg|&-X^T\mathcal{D}\Psi(t_p)+a(t_p)\mathcal{X}^T\Psi(t_p)+b(t_p)\mathcal{U}^T\Psi(t_p)\\&\qquad+\frac{t_i}{2}\sum_{j=0}^{\mathcal{N}}\mathcal{W}_j\left(\mathcal{K}(t_p,\frac{t_i}{2}(\tau_j+1))\varphi\left(X^T\Psi\left(\frac{t_i}{2}(\tau_j+1)\right)\right)\right)\Bigg|\le(M-2)^{\frac{3}{2}-l}\end{aligned}\tag{20}$$

In (20), note that for a given k, as M approaches infinity, the difference between (20) and (16) diminishes because l is at least 2. Thus, the OCP is converted into an NLP with (20) and $\mathcal{X}^T\Psi(0)=x_0$ as constraints and (19) as the objective functional. In this paper, we have utilized the PSO method [15] to solve the discretized OCP. This problem is summarized as follows:

Problem $\overline{\mathcal{P}}$: Find the vectors of X and U that minimize

$$\mathcal{J}_N=\frac{1}{2}\sum_{i=1}^{\mathcal{N}}\mathcal{F}\left(\frac{\tau_j+1}{2},X^T\Psi\left(\frac{\tau_j+1}{2}\right),U^T\Psi\left(\frac{\tau_j+1}{2}\right)\right)\mathcal{W}_j.\tag{21}$$

subject to

$$\begin{aligned}\Bigg|&-X^T\mathcal{D}\Psi(t_p)+a(t_p)\mathcal{X}^T\Psi(t_p)+b(t_p)\mathcal{U}^T\Psi(t_p)\\&\qquad+\frac{t_i}{2}\sum_{j=0}^{\mathcal{N}}\mathcal{W}_j\left(\mathcal{K}(t_p,\frac{t_i}{2}(\tau_j+1))\varphi\left(X^T\Psi\left(\frac{t_i}{2}(\tau_j+1)\right)\right)\right)\Bigg|\le(M-2)^{\frac{3}{2}-l},\end{aligned}\tag{22}$$

and

$$X^T\Psi(0)=0.\tag{23}$$

In this manner, the OCP governed by VIDE is transformed into an NLP. PSO is utilized to solve this NLP.

3.2. NLP solver algorithm

PSO is a prominent optimization algorithm formulated by Dr. Eberhart and Kennedy in 1995 [13, 5]. The algorithm draws inspiration from the collective behavior witnessed in natural phenomena, including the flocking of birds and the schooling of fish. The PSO algorithm commences by initializing a swarm of particles, with each particle representing a candidate solution to the optimization problem under consideration. These particles traverse the solution space by adhering to rules influenced by their personal best positions and the global best position identified by the swarm.

Initially, a set of particles is generated with random positions and velocities within the solution space. Each particle's position corresponds to a potential solution, while the velocities are typically assigned small random values. The fitness of each particle is then assessed using the objective function of the optimization problem.

For each particle, the algorithm compares the current fitness value with its personal best fitness value ($pBest$). If the current fitness is superior, the $pBest$ is updated to the current position. The global best ($gBest$) position, representing the highest fitness value in the swarm, is also determined.

The particle velocities and positions are updated using the following equations:

$$v_i(t+1) = w \cdot v_i(t) + c_1 \cdot r_1 \cdot (pBest_i - x_i(t)) + c_2 \cdot r_2 \cdot (gBest - x_i(t)) \tag{24}$$

$$x_i(t+1) = x_i(t) + v_i(t+1) \tag{25}$$

where $v_i(t)$ is the velocity of particle i at time t, $x_i(t)$ is the position of particle i at time t, w is the inertia weight, c_1 and c_2 are cognitive and social coefficients, respectively, and r_1 and r_2 are random numbers between 0 and 1. These steps are repeated until a stopping criterion is met, such as achieving a maximum number of iterations or attaining a satisfactory fitness level.

PSO's performance is influenced by various parameters, including population size, inertia weight, cognitive coefficient, and social coefficient. The population size determines the number of particles in the swarm; a larger size may enhance exploration but increase computational costs. The inertia weight influences how particles maintain their previous velocities, where a higher value promotes exploration and a lower value promotes exploitation. The cognitive coefficient impacts how much a particle is influenced by its personal best position, while the social coefficient affects the influence of the global best position.

PSO boasts several advantages, such as simplicity, efficiency, and robustness. It is straightforward to understand and implement, capable of swiftly finding good solutions, and effective for diverse optimization problems. Nonetheless, it has drawbacks, including the risk of becoming trapped in local optima and sensitivity to parameter settings, which require careful tuning for optimal performance.

To demonstrate PSO's practical application, consider a scenario where it is used to optimize a complex, nonlinear function with multiple variables. The algorithm starts by initializing a swarm of particles with random positions and velocities. Through iterative updates, the particles gradually converge towards the global best position, representing the optimal solution. This process showcases PSO's capability to efficiently explore and exploit the solution space, making it suitable for the optimization problem discussed in this paper.

Given the complex and nonlinear nature of the optimization problem presented in Section 3, PSO is an excellent choice due to its adaptability and efficiency. The problem involves finding an optimal solution in a high-dimensional space, which PSO can handle effectively through its collaborative search mechanism. Moreover, PSO's ability to converge rapidly to a near-optimal solution makes it suitable for applications where computational resources and time are critical factors.

In conclusion, PSO is selected for its simplicity, robustness, and proven track record in efficiently solving similar optimization problems. The algorithm's flexibility also allows for further refinement and customization which is better to suit the specic requirements of the problem at hand. Here is a step-by-step description of the PSO algorithm for solving the optimization problem:

Initialization

The initialization step in the PSO algorithm involves creating a population of N particles, each with a random initial position x_i and a random initial velocity v_i. The position and velocity are typically initialized within predefined bounds. Additionally, several parameters are set at this stage, including the inertia weight w, cognitive coefficient c_1, social coefficient c_2, and the maximum number of iterations T. These parameters play crucial roles in controlling the behavior and convergence of the algorithm.

Evaluation

The evaluation step involves assessing the fitness of each particle in the swarm. The fitness function $f(x_i)$ evaluates the effectiveness of a particle's position in addressing the optimization problem. Each particle's fitness is calculated based on its current position x_i. This fitness value is used to determine the particle's performance and guide its movement in subsequent iterations.

Update Personal Best
In the update personal best step, each particle's personal best position, denoted as $pBest_i$, is updated. If a particle's current fitness $f(x_i)$ is better than its previous personal best fitness $f(pBest_i)$, the personal best position is updated to the current position, i.e., $pBest_i = x_i$. This allows the particle to remember its best-found position and use it to influence its future movements.

Update Global Best
The update global best step involves identifying the particle with the best fitness value in the swarm. This position is referred to as the global best position $gBest$. The algorithm compares the fitness values of all particles and updates $gBest$ to the particle's position with the best fitness. This global best position is as a reference point for all particles, guiding the swarm towards the optimal solution.

Update Velocity and Position
In this step, the velocity and position of each particle are updated based on its personal best position and the global best position. The new velocity $v_i(t+1)$ is calculated using the formula:

$$v_i(t+1) = w \cdot v_i(t) + c_1 \cdot r_1 \cdot (pBest_i - x_i(t)) + c_2 \cdot r_2 \cdot (gBest - x_i(t)), \tag{26}$$

where r_1 and r_2 are random numbers uniformly distributed in [0, 1]. The new position $x_i(t+1)$ is then updated using the formula:

$$x_i(t+1) = x_i(t) + v_i(t+1). \tag{27}$$

This process allows particles to explore the solution space by adjusting their velocities and positions based on their own experiences and the experiences of the swarm.

Termination
The termination step is the final step of the PSO algorithm. The process of evaluating fitness, updating personal bests, updating the global best, and updating velocities and positions is repeated iteratively until a stopping criterion is met. The stopping criterion can be reaching the maximum number of iterations T or achieving a satisfactory fitness level. Once the termination condition is satisfied, the algorithm outputs the best-found solution, which corresponds to the global best position $gBest$. The flowchart of PSO is given in figure 1.

The flexibility and robustness of PSO make it a suitable choice for a wide range of optimization problems, including those with complex, nonlinear, and high-dimensional solution spaces. This algorithm's proven effectiveness in various applications ensures that it can provide reliable and efficient solutions for the optimization problem described in this paper.

4. Theoretical consideration

Theorems 4.1 and 4.2 establish the uniform convergence and accuracy estimation properties of Chebyshev wavelet expansions. These results provide a strong theoretical foundation forusing of Chebyshev wavelets in approximating functions and solving differential equations. The uniform convergence theorem guarantees that as the number of wavelet terms increases, the approximation error converges to zero uniformly on the interval of interest. Furthermore, the accuracy estimation theorem quantifies convergence rate, allowing for precise error bounds to be determined based on the smoothness of the function being approximated.

Theorem 4.1 ([24]). *A function $\mathcal{G}(t)$, in which second derivative is bounded second, can be approximated by an infinite series of Chebyshev wavelets. This series converges uniformly to the function $\mathcal{G}(t)$, such that,*

$$\mathcal{G}(t) = \sum_{n=1}^{\infty} \sum_{m=0}^{\infty} \mathcal{C}_{nm} \Psi_{nm}(t), \qquad t \in [0,1),$$

in which $\mathcal{C}_{nm} = \langle \mathcal{G}(t), \Psi_{nm}(t) \rangle_{\mathcal{W}_n}$.

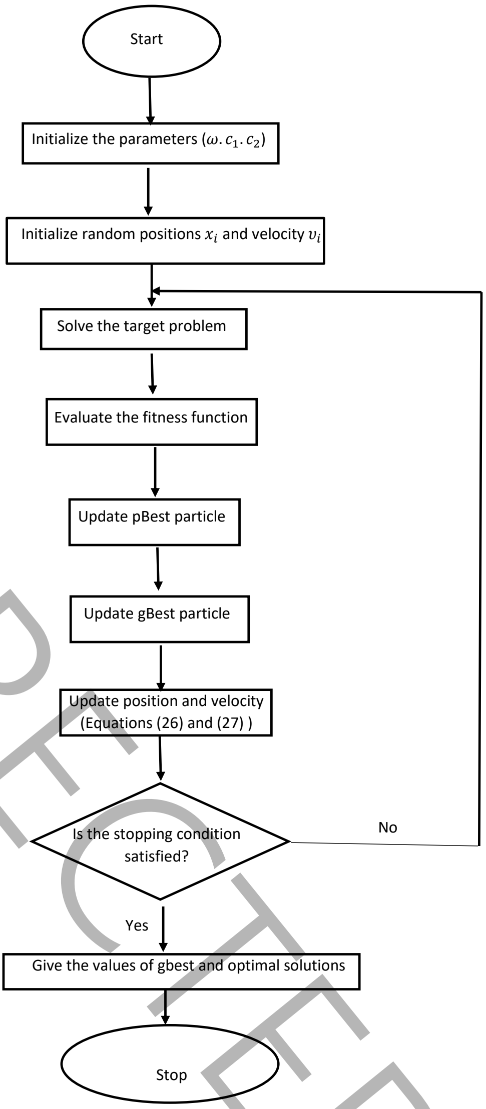
Start
Initialize the parameters $(\omega . c_1 . c_2)$
Initialize random positions x_i and velocity v_i
Solve the target problem
Evaluate the fitness function
Update pBest particle
Update gBest particle
Update position and velocity (Equations (26) and (27))
Is the stopping condition satisfied?
No
Yes
Give the values of gbest and optimal solutions
Stop

Figure 1: The flowchart of PSO for solving the proposed NLP.

Theorem 4.2 (Accuracy Estimation [24]). *Let $\mathcal{G}(t)$ be a continuous function defined on the interval $[0, 1)$ that possesses a bounded second derivative, as outlined in Theorem 4.1. The following accuracy estimation holds:*

$$\left\| \mathcal{G}(t) - \sum_{n=1}^{2^k-1} \sum_{m=0}^{M-1} \mathcal{C}_{n,m} \Psi_{n,m}(t) \right\|_2 < \frac{\sqrt{\pi}\widehat{\mathcal{A}}}{8} \left(\sum_{2^k+1}^{\infty} \frac{1}{n^5} \sum_{m=M}^{\infty} \frac{1}{(m-1)^4} \right)^{\frac{1}{2}},$$

where $\widehat{\mathcal{A}}$ represents the upper bound of the second derivative $\mathcal{G}(t)$.

To validate the convergence analysis, the following two questions need to be addressed:

1. If the problem $\mathcal{P}$ has feasible solution, is the discretized problem $\overline{\mathcal{P}}$ has also feasible solution?
2. Does a sequence of optimal solutions to the discrete problem $\overline{\mathcal{P}}$ converge to the optimal solutions of the original problem $\mathcal{P}$ as the number of Chebyshev wavelet bases increases?

Theorem 4.4 and Theorem 4.5 provide answers to these questions. Before proceeding further, it is necessary to establish some foundational definitions and supporting statements to serve as the basis for the subsequent discussion.

Definition 4.3. *A function $\mathcal{G} : [0,1] \to \Re$ is in Sobolev space $\mathcal{H}^{l,s}$, if its jth distributional derivative, $\mathcal{G}^{(j)}$, lies in $L^s[0,1]$ for all $0 \le j \le l$ with the norm [3]*

$$||\mathcal{G}||_{\mathcal{H}^{l,s}} = \sum_{j=0}^{l} ||\mathcal{G}^{(j)}||_{L^s}, \tag{28}$$

where $||\mathcal{G}||_{L^s}$ denote the usual Lebesgue norm which is defined for $1 \le s < \infty$ as follows:

$$\|\mathcal{G}\|_{L^s} = \Big(\int_0^1 |\mathcal{G}(t)|^s dt \Big)^{\frac{1}{s}},$$

and for $s = \infty$

$$\|\mathcal{G}(t)\|_{L^\infty} = \inf\{\widehat{\mathcal{B}} \ge 0 : |\mathcal{G}(t)| \le \widehat{\mathcal{B}} \text{ for almost every } t \in [0,1]\}.$$

Lemma 4.4 ([3]). *Given any function $\mathcal{G}(t) \in \mathcal{H}^{l,\infty}$, there exists a polynomial $\mathcal{S}_M$ of degree M or less such that*

$$\Big|\mathcal{G}(t) - \mathcal{S}_M(t)\Big| \le CC_0M^{-l}, \quad \forall t \in [0,1],$$

where C is a constant independent of M, l is the order of smoothness of $\mathcal{G}$, and $C_0 = \|f\|_{\mathcal{H}^{l,\infty}}$. The polynomial $\mathcal{G}_M(t)$ with the smallest norm $\|\mathcal{G}(t) - \mathcal{S}_M\|_{L^\infty}$ is referred to as the M-th order best polynomial approximation of $f(t)$ in the L^∞ norm.

Lemma 4.5 ([3]). *Let t_i for $i = 1, \dots, 2^kM$ be LG nodes and $\mathcal{W}_j$ be the LG weights. Assume that $\mathcal{G}(t)$ is Riemann integrable. Then*

$$\int_{-1}^{1} \mathcal{G}(t)\, dt = \lim_{Mk \to \infty} \sum_{i=1}^{2^kM} \mathcal{G}(t_i)\mathcal{W}_j. \tag{29}$$

Remark 4.6. *Evidently, the computational interval can be transformed from $[-1,1]$ to $[a,b]$ via an affine transformation.*

Let

$$\mathcal{X}^* = \big[\mathcal{X}^*_{10}, \mathcal{X}^*_{11}, \dots, \mathcal{X}^*_{2^kM-1}\big]^T \quad \text{and} \quad \mathcal{U}^* = \big[\mathcal{U}^*_{10}, \mathcal{U}^*_{11}, \dots, \mathcal{U}^*_{2^kM-1}\big]^T$$

be the optimal solutions of the problem $\overline{\mathcal{P}}$. The approximate optimal control and state are

$$\overline{\mathcal{X}}^*(t) = \sum_{n=1}^{2^k} \sum_{m=0}^{M-1} \mathcal{X}^*_{nm}\Psi_{nm}(t), \quad \overline{\mathcal{U}}^*(t) = \sum_{n=1}^{2^k} \sum_{m=0}^{M-1} \mathcal{U}^*_{nm}\Psi_{nm}(t).$$

Assume that the following conditions are satisfied:

$\widehat{\mathcal{H}_1}$: The function sequence $\{(\overline{\mathcal{X}}'^*(t), \overline{\mathcal{U}}'^*(t))\}_{M=M'}^{\infty}$ has a subsequence that uniformly converges to the continuous functions $\{(\mathcal{P}^n_{M-2}(t), \mathcal{Q}^n_{M-2}(t))\}$ on each interval $\mathcal{I}_n = [\frac{n-1}{2^k}, \frac{n}{2^k})$ for $1 \le n \le 2^k$. For simplicity in Theorems 4.7 and 4.8 and without loss of generality, we assume that $\{(\overline{\mathcal{X}}'^*(t), \overline{\mathcal{U}}'^*(t))\}_{M=M'}^{\infty}$ converges uniformly to the continuous functions $\{(\mathcal{P}^n_{M-2}(t), \mathcal{Q}^n_{M-2}(t))\}$ on each interval $\mathcal{I}_n$.

$\widehat{\mathcal{H}_2}$: Define

$$\widehat{x}(t) = \int_{\frac{n-1}{2^k}}^{t} \mathcal{P}^n_{M-2}(\tau)\, d\tau + \widehat{x}(\frac{n-1}{2^k}), \quad t \in \mathcal{I}_n, \quad 1 \le n \le 2^k, \tag{30}$$

$$\widehat{u}(t) = \int_{\frac{n-1}{2^k}}^{t} \mathcal{Q}^n_{M-2}(\tau)\, d\tau + \widehat{u}(\frac{n-1}{2^k}), \quad t \in \mathcal{I}_n, \quad 1 \le n \le 2^k. \tag{31}$$

It is presumed for $1 \le n \le 2^k$

$$\lim_{M \to \infty} \overline{\mathcal{X}}^*(\frac{n-1}{2^k}) = \widehat{x}(\frac{n-1}{2^k}), \quad \lim_{M \to \infty} \overline{\mathcal{U}}^*(\frac{n-1}{2^k}) = \widehat{u}(\frac{n-1}{2^k}). \tag{32}$$

$\widehat{\mathcal{H}_3}$: The operator φ is Lipschitz with respect to function u, with Lipschitz constant $\mathcal{L}_\varphi$

$$\Big|\varphi(u_1) - \varphi(u_2)\Big| \le \mathcal{L}_\varphi\big|u_1 - u_2\big|, \quad \forall u_1, u_2 \in U. \tag{33}$$

$\widehat{\mathcal{H}_4}$: Let

$$\max\left\{\left|\mathcal{K}(t,s)\right|, \quad t,s\in[0,1]\right\} = \overline{\mathcal{K}}. \tag{34}$$

$\widehat{\mathcal{H}_5}$: Let

$$\max\left\{|a(t)|, \quad t\in[0,1]\right\} = \mathcal{A}, \quad \max\left\{|b(t)|, \quad t\in[0,1]\right\} = \mathcal{B}. \tag{35}$$

The proofs of the two following theorems are similar to the proof of Theorem 3 and 4 in [9]. Therefore, we omit the details here for brevity.

Theorem 4.7. *Let $(x(t),u(t))$ be feasible solutions of the OCP named $\mathcal{P}$, suppose that $x(t)$ and $u(t)$ belong to $\mathcal{H}^{l,\infty}$ in which $l \geq 2$. If the conditions $\widehat{\mathcal{H}_3}$, $\widehat{\mathcal{H}_4}$, and $\widehat{\mathcal{H}_5}$ are satisfied, then there exists a positive integer M' such that for any $M \geq M'$, the problem $\overline{\mathcal{P}}$ has a feasible solution $(\overline{\mathcal{X}}_p,\overline{\mathcal{U}}_p) = (\overline{\mathcal{X}}(t_p),\overline{\mathcal{U}}(t_p))$, where for $t_p \in \mathcal{I}_n = \left[\frac{n-1}{2^k},\frac{n}{2^k}\right)$, $n = 1,2,\dots,2^k$, the feasible solutions satisfy*

$$|x(t_p) - \overline{\mathcal{X}}_p| \leq \frac{1}{2^k}\mathcal{C}_1^n(M-2)^{1-l}, \quad p = 1,\dots,2^{k-1}M,$$

and

$$|u(t_p) - \overline{\mathcal{U}}_p| \leq \frac{1}{2^k}\mathcal{C}_2^n(M-2)^{1-l}, \quad p = 1,\dots,2^{k-1}M,$$

in which t_p are the GC or GL nodes, and $\mathcal{C}_1^n > 0$ and $\mathcal{C}_2^n > 0$ are constants. [9].

Theorem 4.8. *Let the sequence of optimal solutions to the problem $\overline{\mathcal{P}}$ be represented as*

$$\left\{(\overline{X}(t_p),\overline{U}(t_p)) : (1 \leq p \leq 2^kM),\ k \in N\right\}_{M=M'}^{\infty}.$$

Given that the conditions $\widehat{\mathcal{H}_1}$ and $\widehat{\mathcal{H}_2}$ are satisfied, the pair $(\widehat{x}(t),\widehat{u}(t))$ is recognized as the optimal solution to the problem $\mathcal{P}$ [9].

5. Numerical Assessments

In the numerical experiment section, we utilize the propounded scheme to dissolve the following numerical examples. The numerical results are obtained for $k = 2$ and various values for M. The purpose of solving these examples is to demonstrate the effectiveness and precision of the presented approach. All numerical experiments are done using Mathematica software, which allows us to implement the algorithm and visualize the results efficiently. The examples chosen can test the versatility of the proposed approach. We carefully select parameter values to challenge the method and ensure its robustness.

Example 5.1. *Regard the following OCP*

$$\mathcal{J}(t,x(t),u(t)) = \int_0^1 \Big((x(t)-t)^2 + (u(t)-(1-te^{t^2}))^2\Big)dt, \tag{36}$$

constrained by a nonlinear VID system

$$x'(t) - x(t) - u(t) + 2\int_0^t \Big(tse^{-x^2(s)}\Big)ds = 0, \quad x(0) = 0. \tag{37}$$

The optimal value of cost functional, control $u^*(t)$ and corresponding state $x^*(t)$ are as follows:

$$\begin{cases} \mathcal{J}^* = 0, \\ x^*(t) = t, \\ u^*(t) = 1 - te^{-t^2}. \end{cases} \tag{38}$$

To solve this problem, the functions $x(t)$ and $u(t)$ are approximated using Chebyshev wavelets, and the PSO algorithm is applied to solve the resulting NLP. This method demonstrated that the combination of Chebyshev wavelets and PSO can provide accurate results in solving such problems.

The results of this example clearly show the accuracy of the proposed method, as the absolute error decreases for different values of M and gradually tends towards zero. These results indicate that the proposed method is capable of providing a good approximation of the optimal state and control functions.

Finally, the comparison graphs between the exact and approximate solutions in figure 2 at $M = 8$ and $k = 2$ showed that the approximate solution becomes closer to the exact solution as M increases. This highlights the capability of the proposed method in solving complex OCPs. Tables 1 and 2 show the results of example 5.1 with the combination of Chebyshev wavelet collocation approach and PSO.

Table 1: Obtained absolute errors for $x(t)$ in example 5.1

t	$M=4$	$M=6$	$M=8$
0.0	1.5723×10^{-05}	1.3700×10^{-07}	7.8350×10^{-18}
0.1	1.3806×10^{-05}	3.2124×10^{-08}	9.0515×10^{-10}
0.2	8.1141×10^{-06}	4.9260×10^{-08}	1.4788×10^{-09}
0.3	8.7672×10^{-06}	7.5011×10^{-08}	1.0527×10^{-09}
0.4	1.2809×10^{-05}	2.2095×10^{-08}	1.6969×10^{-09}
0.5	1.4748×10^{-05}	6.3955×10^{-08}	4.5620×10^{-11}
0.6	9.4016×10^{-06}	1.1427×10^{-08}	1.1100×10^{-11}
0.7	7.6742×10^{-06}	2.4253×10^{-08}	3.3173×10^{-11}
0.8	3.6537×10^{-06}	5.7932×10^{-09}	2.4951×10^{-11}
0.9	8.3069×10^{-06}	4.7182×10^{-09}	1.7504×10^{-11}

Table 2: Absolute error of $u(t)$ for example 5.1

t	$M=4$	$M=6$	$M=8$
0	1.40731×10^{-04}	1.0231×10^{-06}	5.9729×10^{-09}
0.1	1.78258×10^{-04}	1.3430×10^{-06}	3.3755×10^{-09}
0.2	1.84659×10^{-04}	7.5561×10^{-07}	8.1428×10^{-10}
0.3	1.60894×10^{-04}	4.9309×10^{-07}	7.4108×10^{-10}
0.4	2.50653×10^{-04}	1.2844×10^{-06}	4.6904×10^{-09}
0.5	2.54043×10^{-04}	1.2289×10^{-06}	3.4729×10^{-09}
0.6	1.70449×10^{-04}	3.4468×10^{-07}	6.9618×10^{-10}
0.7	1.18385×10^{-04}	6.6231×10^{-08}	6.6726×10^{-10}
0.8	1.20167×10^{-04}	2.5800×10^{-07}	7.5670×10^{-10}
0.9	1.20911×10^{-04}	3.2924×10^{-07}	1.3888×10^{-09}

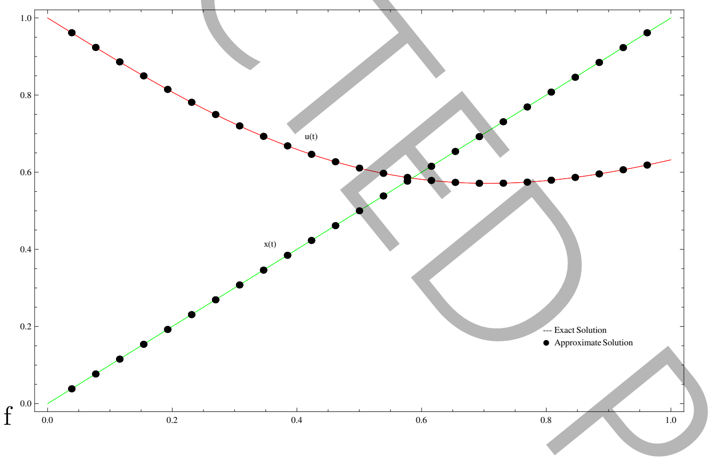

Figure 2: The exact and approximate optimal control and state for example 5.1

Example 5.2. *Consider the minimization of the functional*

$$\mathcal{J}(t,x(t),u(t))=\int_0^1(x(t)-e^t)^2+(u(t)-e^{3t})^2dt, \tag{39}$$

subject to the nonlinear state dynamics

$$x'(t)=\frac{3}{2}x(t)-\frac{1}{2}u(t)+\int_0^t e^{(t-s)}(x(s))^3ds, \quad x(0)=1. \tag{40}$$

The exact optimal control and state are

$$x^*(t)=e^t, \qquad u^*(t)=e^{3t}. \tag{41}$$

To solve this problem, the functions $x(t)$ and $u(t)$ are approximated using Chebyshev wavelets, leading to the transformation of the OCP into an NLP. The wavelet coefficients become the optimization variables, which are then *optimized using the PSO algorithm. The use of Chebyshev wavelets allows for accurate representation of the state and control variables over the defined domain, and the PSO method efficiently explores the solution space to find the optimal solution.*

The numerical results for different values of M show the accuracy of the proposed method. As M increases, the absolute error between the approximate and exact solutions decreases, indicating improved precision. The results are summarized in Tables 3 and 4, which display the absolute errors of the state and control functions for various values of M.

Table 3: The resulted absolute error of $x(t)$ in example 5.2

t	$M = 4$	$M = 6$	$M = 8$
0.0	6.5385×10^{-05}	9.0126×10^{-06}	3.3583×10^{-09}
0.1	1.2988×10^{-04}	4.7235×10^{-06}	1.4326×10^{-09}
0.2	1.5923×10^{-04}	1.2568×10^{-05}	3.7276×10^{-10}
0.3	6.6539×10^{-05}	3.6805×10^{-05}	1.8875×10^{-09}
0.4	1.8014×10^{-05}	3.9821×10^{-05}	9.8288×10^{-10}
0.5	7.4950×10^{-04}	1.0356×10^{-05}	1.1427×10^{-08}
0.6	1.2155×10^{-04}	1.7509×10^{-05}	2.0997×10^{-09}
0.7	7.2211×10^{-05}	1.0744×10^{-05}	3.2806×10^{-09}
0.8	4.3387×10^{-04}	3.5368×10^{-06}	2.4108×10^{-09}
0.9	7.3124×10^{-04}	1.3225×10^{-05}	$2..8436 \times 10^{-09}$

Table 4: The obtained absolute error of function $u(t)$ in example 5.2

t	$M = 4$	$M = 6$	$M = 8$
0.0	$4.4449{\times}10^{-03}$	$4.0180{\times}10^{-04}$	$1.9192{\times}10^{-08}$
0.1	$3.4101{\times}10^{-03}$	$3.0050{\times}10^{-05}$	$1.1596{\times}10^{-08}$
0.2	$1.9417{\times}10^{-03}$	$3.3203{\times}10^{-05}$	$2.8635{\times}10^{-09}$
0.3	$3.0297{\times}10^{-03}$	$3.7617{\times}10^{-04}$	$6.1180{\times}10^{-09}$
0.4	$2.6390{\times}10^{-03}$	$3.1944{\times}10^{-04}$	$2.3350{\times}10^{-08}$
0.5	$1.3558{\times}10^{-02}$	$9.6820{\times}10^{-04}$	$1.2045{\times}10^{-07}$
0.6	$1.2930{\times}10^{-02}$	$3.5890{\times}10^{-04}$	$6.3997{\times}10^{-08}$
0.7	$1.0465{\times}10^{-02}$	$4.5881{\times}10^{-04}$	$1.3786{\times}10^{-09}$
0.8	$1.1714{\times}10^{-02}$	$1.2144{\times}10^{-03}$	$1.7359{\times}10^{-08}$
0.9	$1.4067{\times}10^{-02}$	$1.0453{\times}10^{-03}$	$9.4139{\times}10^{-08}$

Additionally, Figure 3 illustrates the comparison between the exact and approximate solutions for $M = 8$ and $k = 2$. The graph clearly shows that the approximate solutions for the state $x(t)$ and control $u(t)$ converge to their exact counterparts as the number of wavelet terms increases, confirming the robustness and accuracy of the proposed method.

This example highlights the ability of the Chebyshev wavelet collocation method combined with PSO to handle complex, nonlinear dynamics and achieve high accuracy in solving OCPs governed by integro-differential equations. The reduction in absolute error with increasing M demonstrates the potential of this method for tackling similar problems in various fields.

Example 5.3. *Regard the nonlinear OCP*

$$\min \int_0^1 (x(t) - e^{t^2})^2 + (u(t) - (1+2t))^2 dt,$$

subject to nonlinear VIDE

$$x'(t) + x(t) - u(t) - \int_0^t \left(t(1+2t)e^{s(t-s)} \right) ds = 0 \qquad x(0) = 1.$$

in which $u^*(t) = 1+2t$ and $x^* = e^{t^2}$. The obtained errors in the approximate solutions for $k = 2$ and various values of M are shown in tables 5 and 6. The graphs of approximate optimal solutions computed by utilizing Chebyshev

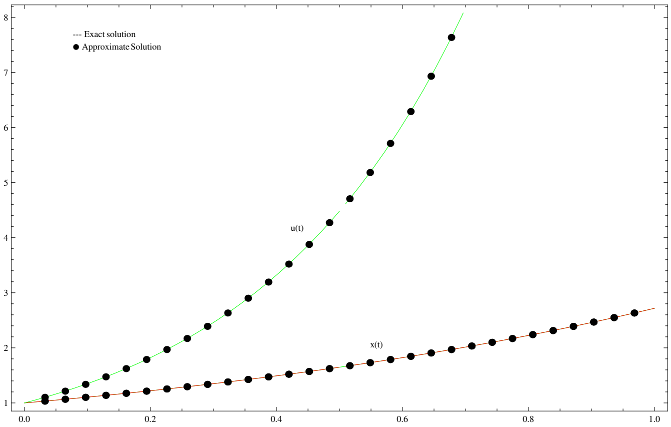

Figure 3: The exact and approximate optimal control and state for example 5.2

wavelet collocation method and PSO are given in figure 4. The resulted absolute errors of the objective functional for examples 5.1, 5.2 and 5.3 are given in table 7. Overall, the results of Example 5.3 indicate that the proposed method, which combines Chebyshev wavelets and the PSO algorithm, provides accurate approximations for both the state and control functions. This example demonstrates the potential of the method in solving complex OCPs involving nonlinear dynamics and integral terms.

Table 5: Absolute error of $x(t)$ for example 5.3

t	$M=4$	$M=6$	$M=8$
0	7.2858×10^{-16}	4.0940×10^{-16}	7.4940×10^{-16}
0.1	2.3075×10^{-4}	5.0007×10^{-6}	5.5132×10^{-9}
0.2	4.0602×10^{-4}	2.9301×10^{-6}	5.8045×10^{-9}
0.3	3.8672×10^{-4}	4.5616×10^{-6}	7.0959×10^{-9}
0.4	3.3456×10^{-4}	1.0447×10^{-5}	8.4205×10^{-9}
0.5	7.4099×10^{-4}	8.2788×10^{-5}	1.0794×10^{-7}
0.6	2.9907×10^{-4}	5.1999×10^{-5}	4.4913×10^{-8}
0.7	2.7521×10^{-3}	7.0772×10^{-5}	3.3385×10^{-8}
0.8	2.7955×10^{-3}	6.6456×10^{-5}	3.3606×10^{-8}
0.9	6.7834×10^{-4}	4.0950×10^{-5}	2.7346×10^{-8}

Table 6: Absolute error of $u(t)$ for example 5.3

t	$M=4$	$M=6$	$M=8$
0	1.7815×10^{-02}	1.7749×10^{-04}	1.2883×10^{-06}
0.1	5.9046×10^{-03}	5.3656×10^{-05}	4.0635×10^{-07}
0.2	4.8001×10^{-03}	3.9358×10^{-05}	3.8180×10^{-07}
0.3	4.7368×10^{-03}	8.0407×10^{-05}	3.4328×10^{-07}
0.4	6.3144×10^{-03}	1.9228×10^{-06}	4.0500×10^{-07}
0.5	8.7257×10^{-02}	1.2305×10^{-03}	1.2060×10^{-05}
0.6	2.9380×10^{-02}	2.2343×10^{-04}	3.7464×10^{-06}
0.7	2.4534×10^{-02}	3.7475×10^{-04}	3.4336×10^{-06}
0.8	2.1832×10^{-02}	3.8713×10^{-04}	3.4007×10^{-06}
0.9	2.9768×10^{-02}	1.7406×10^{-04}	3.7301×10^{-06}

Example 5.4. *Consider minimizing the objective functional given by*

$$\mathcal{J}(t,x(t),u(t)) = \int_0^1 \left[\left(x(t)-(t-\frac{1}{2})\left|t-\frac{1}{2}\right|\right)^2+\left(u(t)-(t-\frac{1}{2})\left|t-\frac{1}{2}\right|\right)^2\right]dt, \tag{42}$$

Table 7: Absolute errors of $\mathcal{J}^*$

M	Example 5.1	Example 5.2	Example 5.3
4	1.0411×10^{-09}	3.2896×10^{-07}	5.18149×10^{-04}
6	4.4257×10^{-14}	2.2842×10^{-09}	7.4609×10^{-08}
8	2.7756×10^{-16}	7.7889×10^{-16}	4.5741×10^{-12}

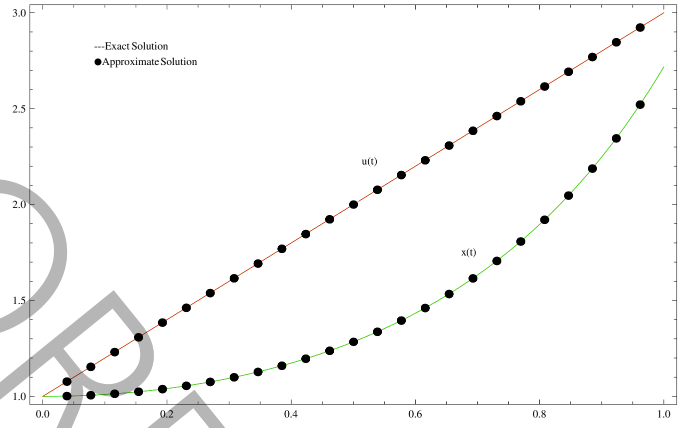

Figure 4: The precise and estimated optimal control and state for 5.3

.

subject to the constraint

$$x(t) = -\frac{t}{32} + (t - \frac{1}{2})\left|t - \frac{1}{2}\right| + \int_0^t \left(x(s) + s^2 u(s)\right) ds. \tag{43}$$

The exact optimal solutions and cost functional are as follows:

$$\begin{gathered} x^*(t) = (t - \tfrac{1}{2})\left|t - \tfrac{1}{2}\right|, \\ u^*(t) = (t - \tfrac{1}{2})\left|t - \tfrac{1}{2}\right|, \\ \mathcal{J}^* = 0. \end{gathered} \tag{44}$$

To solve this problem using our proposed method, we utilize Chebyshev wavelets for approximating the unknown functions $x(t)$ and $u(t)$. By applying the Chebyshev wavelet collocation method, we discretize the system and transform the continuous-time OCP into a NLP problem. The PSO algorithm is then used to solve the derived NLP, where the wavelet coefficients are treated as optimization variables. Table 8 shows the obtained absolute errors in $\mathcal{J}^*$ with the propounded method for different values of k and M. Figures 5 and 6 depict the exact and approximate solutions for example 5.4.

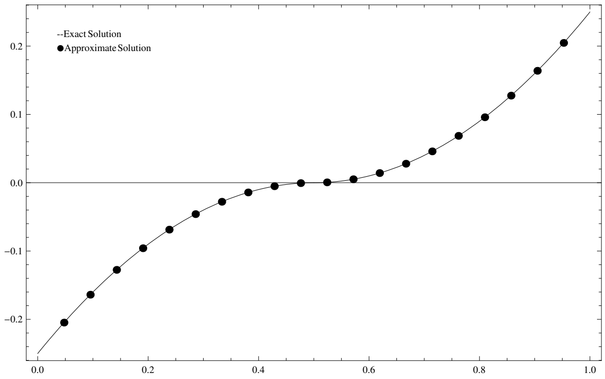

Figure 5: Exact and Approximate optimal control for example 5.4

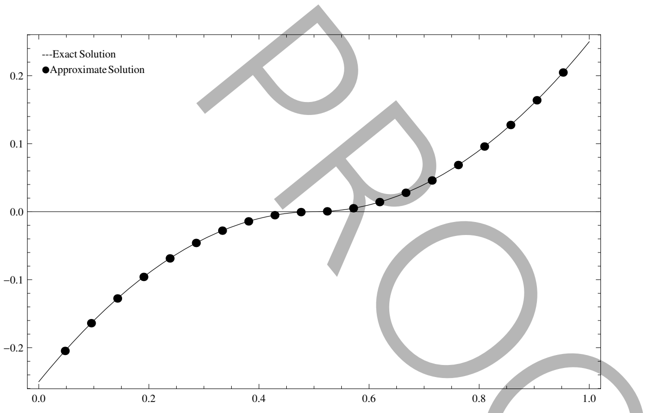

Figure 6: Exact and Approximate optimal state for example 5.4

The outcomes of these examples illustrate the efficacy of the proposed scheme in attaining the optimal control and state. Specifically, the numerical experiments illustrate how the control strategy converges to the optimal solution as we increase the value of M. The results indicate that the proposed approach is reliable and effective for

Table 8: Absolute errors of $\mathcal{J}^*$ for example 5.4

•	$M=3$	$M=4$
$k=2$	3.2877×10^{-9}	3.4807×10^{-10}
$k=3$	1.4796×10^{-11}	1.5638×10^{-12}
$k=4$	6.4946×10^{-14}	8.1601×10^{-15}

addressing optimal control problems governed by variational inequality dynamics (VID). Furthermore, the analysis of the results indicates that as M increases, the approximation of the optimal control and state improves, leading to a reduction in the cost functional $\mathcal{J}$.

6. Concluding Observations

The primary objective of this paper is to introduce a direct methodology for resolving the OCP associated with VID systems. Our approach consists of parameterizing state and control variables and reformulating the OCP into an NLP, wherein the wavelet coefficients are treated as optimization variables. In the numerical experiments presented, using of the operational matrix for differentiation has streamlined the computational process, proving more straightforward than the operational matrix for integration. To solve the derived NLP problem effectively, we employ the Particle Swarm Optimization (PSO) algorithm. PSO, inspired by the social behavior patterns of bird flocking and fish schooling, is well-suited for this problem due to its simplicity, efficient exploration of the search space, and fast convergence rates. The findings demonstrate that the proposed method is efficient and uncomplicated for tackling VID optimal control problems. The synergy of Chebyshev wavelets and PSO offers a robust tool for the optimal control of systems governed by Volterra integro-differential equations, making it applicable across various scientific and engineering disciplines [18]. For future research, the proposed method could be extended to tackle more complex VID systems with time-varying delays and stochastic elements. Additionally, exploring the integration of other metaheuristic algorithms with wavelet-based approaches could further enhance solution accuracy and computational efficiency. For future research, the propounded method could be extended to tackle more complex VID systems with time-varying delays and stochastic elements. Additionally, exploring the integration of other metaheuristic algorithms with wavelet-based approaches could further enhance solution accuracy and computational efficiency.

Acknowledgements

This work has finantional support of Farhangian university (Contract No.500.17474.120).

References

[1] J. T. Betts, *Practical methods for optimal control using nonlinear programming*, vol. 3 of Advances in Design and Control, Society for Industrial and Applied Mathematics (SIAM), Philadelphia, PA, 2001.

[2] J. T. Betts and S. O. Erb, *Optimal low thrust trajectories to the moon*, SIAM J. Appl. Dyn. Syst., 2 (2003), pp. 144–170.

[3] C. Canuto, M. Y. Hussaini, A. Quarteroni, and T. A. Zang, *Spectral methods in fluid dynamics*, Springer Series in Computational Physics, Springer-Verlag, New York, 1988.

[4] M. Diehl, H.-G. Bock, and J. P. Schlöder, *A real-time iteration scheme for nonlinear optimization in optimal feedback control*, SIAM J. Control Optim., 43 (2005), pp. 1714–1736.

[5] R. Eberhart and J. Kennedy, *A new optimizer using particle swarm theory*, in MHS'95. Proceedings of the Sixth International Symposium on Micro Machine and Human Science, 1995, pp. 39–43.

[6] A. Ebrahimzadeh, *A robust method for optimal control problems governed by system of fredholm integral equations in mechanics*, Iran. J. Numer. Anal. Optim., 13 (2023), pp. 243–261.

[7] A. Ebrahimzadeh and E. Hashemizadeh, *Optimal control of non-linear Volterra integral equations with weakly singular kernels based on Genocchi polynomials and collocation method*, J. Nonlinear Math. Phys., 30 (2023), pp. 1758–1773.

[8] M. Ghasemi and M. Tavassoli Kajani, *Numerical solution of time-varying delay systems by Chebyshev wavelets*, Appl. Math. Model., 35 (2011), pp. 5235–5244.

[9] Q. Gong, I. M. Ross, W. Kang, and F. Fahroo, *On the pseudospectral covector mapping theorem for nonlinear optimal control*, in Proceedings of the 45th IEEE Conference on Decision and Control, 2006, pp. 2679–2686.

[10] ——, *Connections between the covector mapping theorem and convergence of pseudospectral methods for optimal control*, Comput. Optim. Appl., 41 (2008), pp. 307–335.

[11] A. Hashemi Borzabadi, A. Abbasi, and O. Solaymani Fard, *Approximate optimal control for a class of nonlinear Volterra integral equations*, J. Amer. Sci, 6 (2010), pp. 1017–1021.

[12] S. G. Hosseini and F. Mohammadi, *A new operational matrix of derivative for Chebyshev wavelets and its applications in solving ordinary differential equations with non analytic solution*, Appl. Math. Sci. (Ruse), 5 (2011), pp. 2537–2548.

[13] J. Kennedy and R. Eberhart, *Particle swarm optimization*, in Proceedings of ICNN'95 - International Conference on Neural Networks, vol. 4, 1995, pp. 1942–1948.

[14] X. Li, F. Xu, and G. Xu, *Redundant Inertial Measurement Unit Reconfiguration and Trajectory Replanning of Launch Vehicle*, Springer Nature Singapore, Singapore, 2023, ch. Optimal Control Problems and Common Solutions, pp. 35–60.

[15] D. G. Luenberger and Y. Ye, *Linear and nonlinear programming*, vol. 116 of International Series in Operations Research & Management Science, Springer, New York, third ed., 2008.

[16] K. Maleknejad and H. Almasieh, *Optimal control of volterra integral equations via triangular functions*, Mathematical and Computer Modelling, 53 (2011), pp. 1902–1909.

[17] K. Maleknejad and A. Ebrahimzadeh, *An efficient hybrid pseudo-spectral method for solving optimal control of Volterra integral systems*, Math. Commun., 19 (2014), pp. 417–435.

[18] K. Maleknejad and A. Ebrahimzadeh, *The use of rationalized Haar wavelet collocation method for solving optimal control of Volterra integral equations*, Journal of Vibration and Control, 21 (2015), pp. 1958–1967.

[19] S. Mashayekhi, Y. Ordokhani, and M. Razzaghi, *Hybrid functions approach for optimal control of systems described by integro-differential equations*, Appl. Math. Model., 37 (2013), pp. 3355–3368.

[20] L. Moradi, D. Conte, E. Farsimadan, F. Palmieri, and B. Paternoster, *Optimal control of system governed by nonlinear Volterra integral and fractional derivative equations*, Comput. Appl. Math., 40 (2021), pp. Paper No. 157, 15.

[21] J. M. Murray, *Optimal control for a cancer chemotherapy problem with general growth and loss functions*, Math. Biosci., 98 (1990), pp. 273–287.

[22] A. Saadatmandi and M. Dehghan, *A new operational matrix for solving fractional-order differential equations*, Comput. Math. Appl., 59 (2010), pp. 1326–1336.

[23] Y. Shi and R. Eberhart, *A modified particle swarm optimizer*, in 1998 IEEE International Conference on Evolutionary Computation Proceedings. IEEE World Congress on Computational Intelligence (Cat. No.98TH8360), 1998, pp. 69–73.

[24] S. Sohrabi, *Comparison Chebyshev wavelets method with bpfs method for solving Abel's integral equation*, Ain Shams Engineering Journal, 2 (2011), pp. 249–254.

[25] E. Tohidi and O. R. N. Samadi, *Optimal control of nonlinear Volterra integral equations via Legendre polynomials*, IMA J. Math. Control Inform., 30 (2013), pp. 67–83.

[26] F. Yassin, Z. Ali, A. Asma, and B. A. Ridha, *Enhancement neural control scheme performance using PSO adaptive rate: experimentation on a transesterification reactor*, J. Vib. Control, 29 (2023), pp. 3769–3782.

[27] Y. Zhang, A. Chi, and S. Mirjalili, *Enhanced jaya algorithm: A simple but efficient optimization method for constrained engineering design problems*, Knowledge-Based Systems, 233 (2021), p. 107555.

Please cite this article using:

Asiyeh Ebrahimzadeh, Solving the optimum control problem constrained with Volterra integro-differential equations using Chebyshev wavelets and particle swarm optimization, AUT J. Math. Comput., 7(1) (2026) 45-61
https://doi.org/10.22060/AJMC.2024.23406.1254